Extracting Quantitative Measures from EAP: A Small Clinical Study Using BFOR

A. Pasha Hosseinbor, Moo K. Chung, Yu-Chien Wu, John O. Fleming, Aaron S. Field, and Andrew L. Alexander

University of Wisconsin-Madison, Madison, WI, USA
hosseinbor@wisc.edu

Abstract. The ensemble average propagator (EAP) describes the 3D average diffusion process of water molecules, capturing both its radial and angular contents, and hence providing rich information about complex tissue microstructure properties. Bessel Fourier orientation reconstruction (BFOR) is one of several analytical, non-Cartesian EAP reconstruction schemes employing multiple shell acquisitions that have recently been proposed. Such modeling bases have not yet been fully exploited in the extraction of rotationally invariant q-space indices that describe the degree of diffusion anisotropy/restrictivity. Such quantitative measures include the zero-displacement probability (Po), mean squared displacement (MSD), q-space inverse variance (QIV), and generalized fractional anisotropy (GFA), and all are simply scalar features of the EAP. In this study, a general relationship between MSD and q-space diffusion signal is derived and an EAP-based definition of GFA is introduced. A significant part of the paper is dedicated to utilizing BFOR in a clinical dataset, comprised of 5 multiple sclerosis (MS) patients and 4 healthy controls, to estimate Po, MSD, QIV, and GFA of corpus callosum, and specifically, to see if such indices can detect changes between normal appearing white matter (NAWM) and healthy white matter (WM). Although the sample size is small, this study is a proof of concept that can be extended to larger sample sizes in the future.

1 Introduction

The aim of diffusion-weighted imaging (DWI) is to non-invasively estimate information about the diffusion of water molecules in biological tissues. The most common form of DWI is diffusion tensor imaging (DTI) [4], which is a good model of diffusion-weighted signal behavior at low levels of diffusion weighting. Rotationally invariant measures can be derived from the eigenvalues of the diffusion tensor, including fractional anisotropy (FA) and mean diffusivity (MD) [5], that have proven clinical value. However, DTI is limited by the Gaussian assumption, which is invalid at higher levels of diffusion weighting ($b > 2000$ s/mm^2) and its inability to resolve multiple fiber orientations within a voxel [12].

In order to recover complex white matter (WM) geometry, high angular resolution diffusion imaging (HARDI) [12], which reduces the diffusion signal sampling to a single sphere (i.e. single level of diffusion weighting) within q-space,

N. Ayache et al. (Eds.): MICCAI 2012, Part II, LNCS 7511, pp. 280–287, 2012.

was proposed. Many HARDI techniques [7, 11] seek to extract the orientation distribution function (ODF), a probability density function describing the angular distribution of water molecules during diffusion. However, the ODF only retrieves the angular content of the diffusion process.

The ensemble average propagator (EAP) provides the full information about the diffusion process in the tissue because it captures both the radial and angular information contained in the diffusion signal. The ODF is simply an angular feature of the EAP. Unlike the diffusion tensor, the EAP profiles illustrate and recover crossing fibers. The significance of the EAP in diffusion MRI has led to many reconstruction algorithms being proposed, some numerically based such as diffusion specturm imaging (DSI) [13] and hybrid diffusion imaging (HYDI) [16], and some analytically based such as diffusion propagator imaging (DPI) [9], spherical polar Fourier imaging (SPFI) [3, 8], and Bessel Fourier orientation reconstruction (BFOR) [10].

With respect to analytical EAP reconstruction methods, one valuable though overlooked use is in extracting rotationally invariant quantitative measures from them. High angular resolution analogues of quantitative DTI indices such as generalized fractional anisotropy (GFA) [11] & mean squared displacement (MSD) [2, 16] and other q-space metrics like zero-displacement probablity (Po) [2] & q-space inverse variance (QIV) [17] are all scalar features of the EAP. Analytical representations of the EAP (and hence diffusion signal) facillitate either analytic computation of such features or numerical efficiency in estimating them. HYDI has already been used to numerically estimate Po, MSD, and QIV [17].

In this paper, we derive analytical expressions for Po, MSD, & QIV using BFOR, and introduce an EAP-based definition of GFA. These quantitative measures are then utilized in a HYDI-acquired clinical dataset, comprising a healthy control group and multiple sclerosis (MS) patients, to see if they detect any differences in the corpus callosum between the normal appearing white watter (NAWM) of MS patients and healthy WM.

2 Theory

Let $P(\mathbf{p})$ and $E(\mathbf{q})$ be the EAP and normalized q-space diffusion signal, respectively. We denote $\mathbf{q} = q\ \mathbf{u}(\theta, \phi)$ and $\mathbf{p} = p\ \mathbf{r}(\theta', \phi')$, where $\mathbf{u}$ and $\mathbf{r}$ are 3D unit vectors. Under the narrow pulse assumption, $E(\mathbf{q})$ and $P(\mathbf{p})$ are Fourier Transform (FT) pairs [6]:

$$P(\mathbf{p}) = \int E(\mathbf{q}) e^{-2\pi i \mathbf{q}\cdot\mathbf{p}} d^3\mathbf{q} \tag{1}$$

The BFOR signal basis and EAP are, respectively,

$$E(\mathbf{q}, t) = \sum_{n=1}^{N} \sum_{j=1}^{R} C_{nj} e^{\frac{-\alpha_{nl(j)}^2 t}{\tau^2}} j_{l(j)}(\frac{\alpha_{nl(j)} q}{\tau}) Y_j(\mathbf{u}) \tag{2}$$

and

$$P(\mathbf{p},t) = 2\tau\sqrt{2\pi^3}\sum_{n=1}^{N}\sum_{j=1}^{R}(-1)^{\frac{l(j)}{2}}C_{nj}e^{\frac{-\alpha_{nl(j)}^2 t}{\tau^2}}Y_j(\mathbf{r})\frac{\sqrt{\alpha_{nl(j)}}J_{l(j)-1/2}(\alpha_{nl(j)})j_{l(j)}(2\pi\tau p)}{\left(4\pi^2p^2-\frac{\alpha_{nl(j)}^2}{\tau^2}\right)}, \tag{3}$$

where $e^{\frac{-\alpha_{nl(j)}^2 t}{\tau^2}}$ is the smoothening term, C_{nj} are the expansion coefficients, and $\alpha_{nl(j)}$ is n^{th} root of l^{th} order spherical Bessel function of first kind j_l [10].

2.1 Rotationally Invariant Quantitative *q*-Space Indices

$Po = P(\mathbf{p} = 0)$ is the probability density of water molecules that minimally diffuse within the diffusion time [2,16], and hence a measure of restricted diffusion. In a healthy adult brain, Po is greater in white matter (WM) than gray matter (GM) because WM has more restricting barriers including multi-layer myelin sheaths, axonal membranes, and microtubules. Several studies have shown Po to be sensitive to brain pathology, and suggesting that changes in myelin are the primary mechanism for differences in Po [1,18].

Po can be evaluated either numerically or analytically. The authors in [17] computed Po by numerically summing the normalized diffusion signal $E(\mathbf{q})$ over all diffusion measurements in q-space, and then correcting the sum by the sampling density. Analytical formulations of Po were derived for the SPFI and DPI signal bases [8,9]. The BFOR Po can be computed analytically by evaluating Eq. (3) at $p = 0$[1]:

$$Po = 2\sqrt{\pi}\tau^3\sum_{n=1}^{N}C_{n1}\frac{(-1)^{n+1}}{\alpha_{n0}^2} \tag{4}$$

The MSD, which we will denote as $\langle p^2\rangle$, is simply the second moment of the EAP [16]: $\langle p^2\rangle = \int p^2 P(\mathbf{p})d^3\mathbf{p}$. It is related to the MD, which in the case of Gaussian diffusion is given by the well-known Einstein relation $\langle p^2\rangle = 6(\Delta - \delta/3)\text{MD}$. Thus far, an analytical formulation of MSD exists only within the DTI framework. It is calculated numerically in q-space imaging, either by extracting the full width at half maximum of the EAP [2] or taking the geometrical mean of the diffusion signal over all directions on a HYDI shell [17]

A general relationship between the MSD and q-space diffusion signal has not yet been formulated to the authors' knowledge. Such a relationship is derived in the **Supplementary Section**:

$$\langle p^2\rangle = \frac{-1}{4\pi^2}\bigtriangledown^2 E(\mathbf{q})|_{\mathbf{q}=0} \tag{5}$$

According to Eq. (5), DPI, which models the diffusion signal as $\bigtriangledown^2 E(\mathbf{q}) = 0$, predicts the MSD to be zero which is unrealistic. Using Eq. (5), an analytic MSD

[1] For all derivations, see `http://brainimaging.waisman.wisc.edu/~ameer/Suppl.pdf`

expression can be computed for BFOR because the BFOR signal basis, Eq. (2), is an eigenfunction of the Laplacian operator. Hence, it can be shown that

$$\langle p^2 \rangle_{BFOR} = \frac{1}{8\pi^{\frac{5}{2}}\tau^2} \sum_{n=1}^{N} C_{n1}\alpha_{n0}^2 \tag{6}$$

The MSD measure is quite sensitive to noise [16]. The authors in [17] proposed an alternative measure to MSD called the QIV, which is a pseudo-diffusivity measure. Mathematically, the QIV is defined as $QIV = \left[\int q^2 E(\mathbf{q}) d^3\mathbf{q}\right]^{-1}$. The QIV is not an arbitrary meausre, but related to the EAP in a manner analogous to which the MSD is related to the diffusion signal-in **Suppl. Section**, we will show that $QIV^{-1} = \frac{-1}{4\pi^2} \bigtriangledown^2 P(\mathbf{p})|_{\mathbf{p}=0}$. The QIV within the BFOR framework is

$$QIV_{BFOR} = \frac{1}{2\sqrt{\pi}\tau^5 \sum_{n=1}^{N}(-1)^n C_{n1} \frac{(6-\alpha_{n0}^2)}{\alpha_{n0}^4}} \tag{7}$$

Tuch in [11] introduced the concept of GFA and defined it as std(ODF)/ rms(ODF). Since ODF is only a feature of the EAP, the subsequent GFA map is derived soley from the angular content of the diffusion profile. Incorporating both the angular and radial contents of the diffusion profile into the definition of GFA will result in a radial dial of GFA maps, illustrating how anisotropy varies with diffusion displacement p. Therefore, we define a new GFA:

$$GFA(p = p_o) = \frac{std\left[P(p = p_o, \mathbf{r})\right]}{rms\left[P(p = p_o, \mathbf{r})\right]} \tag{8}$$

Another advantage of Eq. (8) is that it is better suited for multiple diffusion weighted MR experiments, unlike Tuch's definition, which is HARDI-based.

3 Materials and Methods

The *in vivo* dataset uses a hybrid, non-Cartesian sampling scheme [16], shown in Table 1. Since EAP reconstruction is sensitive to angular resolution, the number of encoding directions is increased with each shell to increase the angular resolution with the level of diffusion weighting. The number of directions in the outer shells were increased to better characterize complex tissue organization.

HYDI was performed on five MS patients and four healthy volunteers using a 3.0 T GE-SIGNA whole body scanner. MR parameters were TE = 99 ms, TR 2300 ms, FOV = 24 cm, matrix = 96 x 96, voxel size = 2.5 x 2.5 mm^2, 15 slices with slice thickness = 5 mm, and scan time = 10 min. Diffusion parameters were Δ = 45 ms, δ = 34 ms, field of view of the diffusion displacement space FOV_p = $(1/\Delta q)$ = 71.4 μm, and resolution of the diffusion displacement space Δp = $(1/2q_{max})$ = 7.1 μm [6].

DTI analysis was performed using the data in the second HYDI shell, in order to obtain the FA and MD, with the FSL software package [15]. BFOR was then used to compute Po, MSD, QIV, and GFA, with model parameters

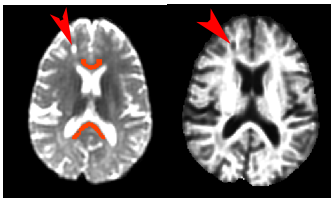

(a) T_2W **(b)** Po

Fig. 1. Axial slice of T_2W and corresponding BFOR Po map illustrating corpus callosum ROI (red) and MS lesion (red arrow).

Table 1. HYDI Encoding Scheme for Human Dataset

Shell	Ne	q (mm^{-1})	Δq (mm^{-1})	b (s/mm^2)
	2	0		0
1st	6	14	14	260
2nd	21	28	14	1040
3rd	24	42	14	2340
4th	24	56	14	4160
5th	50	70	14	6500

set to $\{L = 4, N = 6, \tau = 84$ mm^{-1}, $\lambda_l = 10^{-6}, \lambda_n = 10^{-6}, t = 0\}$. Using the T_2W ($b = 0$ volume) and BFOR Po maps as references, ROIs of the genu and splenium of corpus callosum were then manually drawn for each subject, as shown in Fig. 1, which were also applied to the other quantitative maps. An unpaired two-sample t-test (one-tailed), assuming unequal variances, was then used to test whether the mean value of each index in the corpus callosum for the NAWM group was lower (FA, GFA & Po) or higher (DTI/BFOR MSD & QIV) than those from control group at 0.05 level.

4 Results

Fig. 4 displays axial slices of the BFOR computed Po, QIV, & MSD indices. Note that the QIV exhibits GM/WM contrast, unlike MSD. Within the CSF regions in QIV map, some voxels were zeroed out because they blew up upon the division operation in computing QIV. Fig. 3 shows axial slices of the GFA estimated at $p = 5$, 10, and 15 μm, illustrating how the anisotropy of different WM regions, such as the corpus callosum and capsules, varies with diffusion displacement p. CSF regions in the GFA map at $p = 15$ μm are more noisy than at 5 & 10 μm.

Fig. 2 displays the mean and standard deviation of GFA, MSD, QIV, Po, FA, and DTI MSD for each subject. The t-test yielded a statistically significant p-value between the mean value of each index in NAWM and healthy WM at 0.05 level for GFA(5) & GFA(10) and Po, implying a reduction in GFA and Po of NAWM in corpus callosum with respect to controls. Such findings are consistent with previous DTI [14] and q-space [1] MS studies that showed significant reductions in FA and Po of NAWM with respect to controls, respectively. Although the DTI FA was also statistically significant, the p-values for GFA(5) & GFA(10) are much smaller than for FA, suggesting that GFA may be more sensitive to pathologically induced changes in WM than normal FA. The BFOR MSD was not a statistically significant indicator of pathological changes in WM, which goes against the results of [1,14] that showed MD/MSD to be significantly

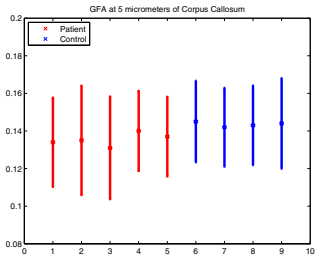

(a) GFA(5); p-value=0.0018

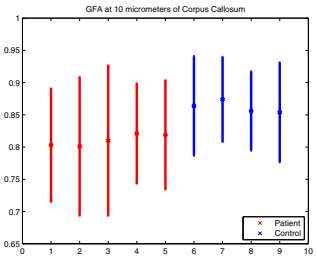

(b) GFA(10); p-value=4.8e-5

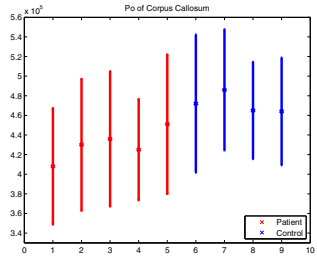

(c) *Po*; p-value=0.0011

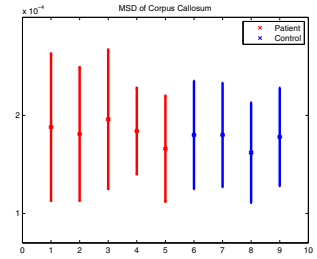

(d) BFOR MSD; p-value=0.13

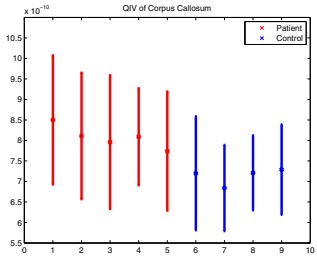

(e) QIV; p-value=3.0e-4

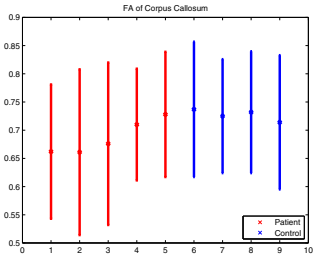

(f) DTI FA; p-value=0.020

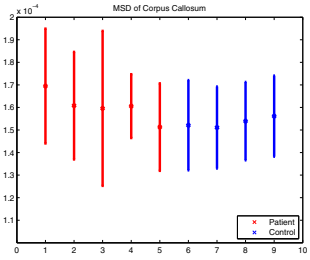

(g) DTI MSD; p-value=0.035

Fig. 2. Mean and stdv. of measures in corpus callosum for each subject, with the p-value of the unpaired two-sample t-test (one-tailed)

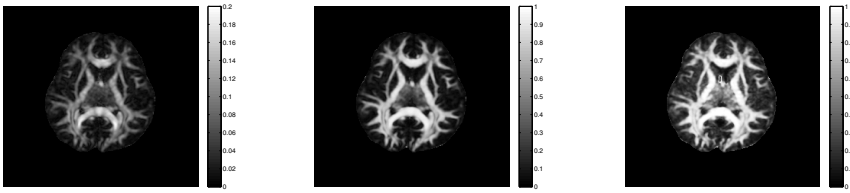

(a) $p = 5$ μm **(b)** $p = 10$ μm **(c)** $p = 15$ μm

Fig. 3. Axial slices of BFOR GFA maps at $p = 5$, 10, and 15 μm for a control

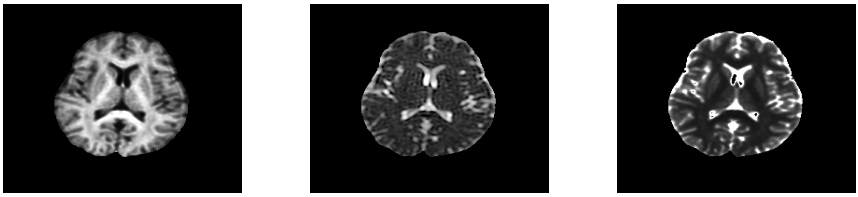

(a) Po **(b)** MSD **(c)** QIV

Fig. 4. Axial slices of BFOR estimated Po, MSD, and QIV maps for a control

higher in NAWM with respect to controls. The DTI MSD, however, was found to be statistically significant, and the disparity in results between the DTI and BFOR MSD may be due to the high b-value (BFOR) MSD being very sensitive to noise [16]. The QIV, however, was found to be significantly higher in NAWM with respect to controls, and both it and GFA(10) had the highest statistical significances among all metrics. In general, the BFOR computed measures validate the main finding of [1], being that q-space indices suggest abnormalities in the MS brain are not only confined to hyerintense lesions visible in T_2 images, but may also affect the surrounding NAWM.

5 Conclusion

This is the first study to date to utilize an analytical, hybrid, and non-Cartesian EAP framework for the computation of rotationally invariant quantitative measures in a clinical dataset. Although the study was limited by the small sample size, it demonstrates the potential that EAP-derived q-space indices have in assessing brain pathology. In the future, the same study should be repeated using a larger sample size, with measurements being made in other WM regions in addition to the corpus callosum. Future work also includes estimating the axial and radial diffusivities using an analytical EAP framework.

References

1. Assaf, Y., Ben Bashat, D., Chapman, J., Peled, S., Biton, I.E., Kafri, M., Segev, Y., Hendler, T., Korczyn, A.D., Graif, M., Cohen, Y.: High b-value q-space analyzed diffusion-weighted MRI: application to multiple sclerosis. Magn. Reson. Med. 47, 115–126 (2002)
2. Assaf, Y., Mayk, A., Cohen, Y.: Displacement imaging of spinal cord using q-space diffusion-weighted MRI. Magn. Reson. Med. 44, 713–722 (2000)
3. Assemlal, H.E., Tschumperlé, D., Brun, L.: Efficient and robust computation of PDF features from diffusion MR signal. Med. Image Anal. 13, 715–729 (2009)
4. Basser, P.J., Mattiello, J., LeBihan, D.: MR diffusion tensor spectroscopy and imaging. Biophysical Journal 66, 259–267 (1994)
5. Basser, P.J., Pierpaoli, C.: Microstructural and physiological features of tissues elucidated by quantitative-diffusion-tensor MRI. J. Magn. Reson. 111, 209–219 (1996)
6. Callaghan, P.T.: Principles of Nuclear Magnetic Resonance Microscopy. Oxford University Press, Oxford (1991)
7. Canales-Rodriguez, E.J., Melie-Garcia, L., Iturria-Medina, Y.: Mathematical description of q-space in spherical coordinates: exact q-ball imaging. Magn. Reson. Med. 61, 1350–1367 (2009)
8. Cheng, J., Ghosh, A., Jiang, T., Deriche, R.: Model-Free and Analytical EAP Reconstruction via Spherical Polar Fourier Diffusion MRI. In: Jiang, T., Navab, N., Pluim, J.P.W., Viergever, M.A. (eds.) MICCAI 2010, Part I. LNCS, vol. 6361, pp. 590–597. Springer, Heidelberg (2010)
9. Descoteaux, M., Deriche, R., LeBihan, D., Mangin, J.F., Poupon, C.: Multiple q-shell diffusion propagator imaging. Med. Image Anal. 15, 603–621 (2011)
10. Hosseinbor, A.P., Chung, M.K., Wu, Y.-C., Alexander, A.L.: Bessel Fourier Orientation Reconstruction: An Analytical EAP Reconstruction Using Multiple Shell Acquisitions in Diffusion MRI. In: Fichtinger, G., Martel, A., Peters, T. (eds.) MICCAI 2011, Part II. LNCS, vol. 6892, pp. 217–225. Springer, Heidelberg (2011)
11. Tuch, D.S.: Q-ball imaging. Magn. Reson. Med. 52, 1358–1372 (2004)
12. Tuch, D.S., Reese, T.G., Wiegell, M.R., Makris, N., Belliveau, J.W., Weeden, V.J.: High angular resolution diffusion imaging reveals intravoxel white matter fiber heterogeneity. Magn. Reson. Med. 48, 577–582 (2002)
13. Weeden, V.J., Hagmann, P., Tseng, W.Y.I., Reese, T.G., Weisskoff, R.M.: Mapping complex tissue architecture with diffusion spectrum magnetic resonance imaging. Magn. Reson. Med. 54, 1377–1386 (2005)
14. Werring, D.J., Clark, C.A., Barker, G.J., Thompson, A.J., Miller, D.H.: Diffusion tensor imaging of lesions and normal-appearing white matter in multiple sclerosis. Neurology 52, 1626–1632 (1999)
15. Woolrich, M.W., Jbabdi, S., Patenaude, B., Chappell, M., Makni, S., Behrens, T., Beckmann, C., Jenkinson, M., Smith, S.M.: Bayesian analysis of neuroimaging data in FSL. NeuroImage 45, 173–186 (2009)
16. Wu, Y.C., Alexander, A.L.: Hybrid diffusion imaging. NeuroImage 36, 617–629 (2007)
17. Wu, Y.C., Field, A.S., Alexander, A.L.: Computation of diffusion function measures in q-space using magnetic resonance hybrid diffusion imaging. IEEE Transac. Med. Imaging 27, 858–865 (2008)
18. Wu, Y.C., Field, A.S., Duncan, I.D., Samsonov, A.A., Kondo, Y., Tudorascu, D., Alexander, A.L.: High b-value and diffusion tensor imaging in a canine model of dysmyelination and brain maturation. NeuroImage 58, 829–837 (2011)